


Article

An Eddy Dissipation Concept Performance Study for Space Propulsion Applications

Daniel Martinez-Sanchis ^{1,*} , Andrej Sternin ^{1,2}, Jaroslaw Shvab ³, Oskar Haidn ¹ and Xiangyu Hu ⁴¹ Department of Space Propulsion, Technical University of Munich, 80333 Munich, Germany² Chair of Space Systems, Technical University of Dresden, 01069 Dresden, Germany³ Global Research for Safety (GRS), Technical University of Munich, 80333 Munich, Germany⁴ Chair of Aerodynamics and Fluid Mechanics, Technical University of Munich, 80333 Munich, Germany

* Correspondence: daniel.martinez@tum.de

Abstract: In this study, Direct Numerical Simulations (DNS) of a turbulent diffusion flame are conducted to investigate the performance of the Eddy Dissipation Concept in turbulent combustion for space propulsion applications. A 20-bar methane-oxygen diffusion flame is simulated to resemble the conditions encountered in modern rocket combustors. The numerical simulations were conducted using the software EBI-DNS within the OpenFOAM framework. An approach for analysis and validation of the combustion model with DNS is developed. The EDC model presents a good agreement with DNS observations in the most prevalent species. Nevertheless, the EDC struggles to predict the mean chemical production rate of intermediate species. It is found that local adaptation of the model constants is essential for maximizing the prediction capabilities. The relationship of these parameters with the Reynolds number and the Damköhler number are mostly in good agreement with the trends proposed in recent research.

Keywords: turbulence; combustion; space propulsion; EDC; DNS



Citation: Martinez-Sanchis, D.; Sternin, A.; Shvab, J.; Haidn, O.; Hu, X. An Eddy Dissipation Concept Performance Study for Space Propulsion Applications. *Aerospace* **2022**, *9*, 476. <https://doi.org/10.3390/aerospace9090476>

Academic Editor: Kevin Lyons

Received: 26 July 2022

Accepted: 24 August 2022

Published: 27 August 2022

Publisher's Note: MDPI stays neutral with regard to jurisdictional claims in published maps and institutional affiliations.



Copyright: © 2022 by the authors. Licensee MDPI, Basel, Switzerland. This article is an open access article distributed under the terms and conditions of the Creative Commons Attribution (CC BY) license (<https://creativecommons.org/licenses/by/4.0/>).

1. Introduction

The combustion chamber of a Liquid Rocket Engine (LRE) plays a central role in the overall performance of the engine. This element enables the complete reaction of the injected propellants along with their atomization, mixing, and vaporization [1–3]. The need for efficient launch vehicles demands the execution of these tasks within the minimum possible length, maximizing mass savings. The design process for such systems strongly is heavily reliant on computerized simulations. In this context, the fluid interface constitutes a remarkable challenge in terms of predictability [4]. Under typical operating conditions in an LRE, density, temperature, and velocity can vary an order of magnitude within a few microns. The physical driving processes in a turbulent reacting flow span over several scales, yielding an exponential growth of the computational cost. Hence, Direct Numerical Simulations (DNS) for entire combustion chambers are prohibitively expensive under today's technological constraints. This high computational cost has motivated the quest for alternatives since the early days of Computational Fluid Dynamics (CFD). The most widely employed solution for industrial applications are statistical models based on Reynolds-Averaged Navier-Stokes (RANS) equations [5]. This sort of models arises after averaging the deterministic Navier Stokes conservation equations over time. This consideration simplifies the problem. First, the resolution requirements are notably lowered since the requisite of resolving all turbulent scales is eliminated. Second, unlike instantaneous fields, statistical fields may be stationary and symmetric, allowing for smaller computational extents. Despite these advantages, operating with statistical terms has important shortcomings. During the averaging process, additional terms originate in the conservation equations formulation. These terms are unclosed and require modeling for their determination. This circumstance is referred to as the closure problem, and it is one

of the greatest unsolved challenges in classical physics. The present paper focuses on the Favre-averaged [6] chemical production rate of the species $\tilde{\omega}_j$, which is one of the unclosed elements in the conservation equation of chemical species for turbulent reacting flows. The averaged chemical production rate originates from the development of combustion in the context of a turbulent flow. This term is central in combustion modeling as it summarizes the influence of turbulence in combustion development. The most extended strategies to approach this term are flamelet models [7] and the Eddy Dissipation Concept (EDC) [8–10]. The present paper focuses on the latter.

The eddy dissipation concept was originally proposed by Magnussen and Hjertager and developed by their research group in the subsequent years. Other authors [11,12] have proposed adaptations to enhance the model's performance in specific combustion regimes. Here, the model is presented in the most general way to provide a common ground for the next section's analysis.

EDC arises as a generalization for the Eddy Dissipation Model (EDM) in the case of detailed chemistry. The main assumption in both methods is that combustion takes place at the Kolmogorov scale in Perfectly Stirred Reactor (PSR) conditions. The structures responsible for combustion are referred to as fine structures, and they have characteristic length and time scales that overlap with those of turbulent structures. More specifically, the fine structures are characterized by a residence time τ^* , a length scale L^* , and a velocity scale u^* . Magnussen [13] argued that the fine structures are placed in isoenergetic regions where the turbulent kinetic energy is characterized by the root mean square (RMS) of the velocity fluctuations u' . Departing from this assumption, the volumetric mass fraction of the fine structures can be estimated as:

$$\gamma^* = \left(\frac{u^*}{u'}\right)^2 \quad (1)$$

Using this result, the length fraction was set as $\gamma_\lambda = \sqrt[3]{\gamma^*}$ [10]. This parameter is modeled to be inversely proportional to the fourth root turbulent Reynolds number Re_T :

$$\gamma_\lambda = C_\gamma \left(\frac{\nu \varepsilon}{k^2}\right)^{\frac{1}{4}} = C_\gamma Re_T^{-1/4} \quad (2)$$

where C_γ is a model parameter. The residence time of the fine structures is usually modelled assuming proportionality with the Kolmogorov timescale:

$$\tau^* = C_\tau \tau_\eta = C_\tau \left(\frac{\nu}{\varepsilon}\right)^{1/2} \quad (3)$$

with C_τ being a model constant. Both C_γ and C_τ provide the main degrees of freedom to the different versions of the EDC models. It is important to note that these degrees of freedom can also be described by the parameters $C_{D1} = (3C_\tau)/(2C_\gamma^2)$ and $C_{D2} = 3C_\tau^2$ instead. Departing from the presented ideas, the EDC derives the following formulation for closure of the mean production rate of a given species:

$$\tilde{\omega}_j = g(\gamma_\lambda, \chi) \bar{\rho} \frac{\tilde{Y}_j^* - \tilde{Y}_j}{\tau^*} \quad (4)$$

where \tilde{Y}_j^* denotes the Favre-averaged mass fraction of the j^{th} species after a time-lapse τ^* under PSR conditions. The parameter χ accounts for the fraction of effectively reacting fine structures. The largest hindrance to achieving generality in the model application is an adequate formulation for the factor $g(\gamma_\lambda, \chi)$. Several definitions have been proposed

depending on the physical considerations. The following expression provides the most general formulation for the coefficient g :

$$g(\gamma_\lambda, \chi) = \frac{\gamma_\lambda^n \chi}{1 - \gamma_\lambda^m \chi} \quad (5)$$

where the exponents n and m are specific for each model version, and they are strongly linked to the physical processes considered during the model derivation. For example, the quadratic dependency in (1) implies an assumption of a tube-like geometry for the fine structures. Assuming a sheet-like structure yields a cubic dependency instead [14]. These sorts of considerations determine the actual values of n and m . The reader is referred to the specialized literature [14–16], where the different EDC versions are discussed along with their phenomenological implications. Besides the mentioned exponents, the main drivers in (5) are the fine structures length fraction γ_λ and the reactivity factor χ . The factor χ accounts for the fraction of fine structures that are effectively reacting, and it was originally taken as unity. Some authors [17] argue that this supposition may not be valid, especially for flows with moderate turbulence levels. There are indeed proposed dependencies of χ on the turbulent Reynolds number [17,18]. Gran and Magnussen [19,20] studied the model's sensitivity to the usage of non-unity values for χ , reporting a marginal effect. The authors discussed that the non-reactivity factor of the species is implicitly determined by the batch reactor part of the model. More specifically, Ertesvåg [14] interpreted their work by arguing that the influence posed by the low presence reactants is already captured in the term $(\tilde{Y}_j^* - \tilde{Y}_j)$ in (4).

In the aforementioned equations, both C_γ and C_τ are considered to be constant. However, recent works from Parente [11] and Bao [12] introduced dependencies on the Damköhler number of the Kolmogorov eddies Da_η and the turbulent Reynolds number Re_τ . These approaches were conceived within the framework of Moderate or Intense Low oxygen Dilution (MILD) combustion. Combustion in this regime is characterized by a widely distributed reaction zone, challenging certain assumptions of the classical EDC conception. This scenario is, in principle, not expected in LRE, at least in the near injection region. However, further downstream, the hypothesis of a widely distributed combustion regime could be reasonable in certain cases.

The main advantage of EDC is its simplicity and easy tuning, which has fostered its widespread application over the last decades. However, the model derivation is strongly dependent on ideal assumptions, which are likely to deviate from the conditions in a real environment. These idealized premises make it difficult to adapt the model for more realistic applications through incorporation of more sophisticated physical processes. Consequently, the adaptation of EDC is often achieved by the variation of the model constants, which can be decoupled from physical processes.

Validation in turbulent flow models can occur at different tiers [21,22]. Ideally, one is able to measure all of the relevant statistics and compare them with the predicted output from the CFD software. However, this process can be quite challenging, even for non-reacting flows. For this reason, validation is often performed at higher tiers, meaning that the validation data does not directly correspond to modeled quantities but is indirectly related to them. This is typically the case in turbulent combustion applications. To this date, the validation of EDC models has mainly been achieved through integral measurements [16]. For example, heat fluxes, temperatures, or radial averages of properties have been taken as ground truth data. The usage of integral quantities as validation parameters is motivated by technical limitations. Although this approach can provide a rough idea of the model's performance, coupling with other modeled effects and physical phenomena arise. These intermediate effects effectively act as interferences and can impair the results' accuracy. For example, errors in the modeled intermediate aspects may require biases in EDC to be compensated. Furthermore, it can be difficult to study the detailed processes in which EDC models are grounded. DNS offers the possibility of observing the local

performance of EDC and the assumptions on which it relies. The time-averaged direct resolution of the flow's conservation equations provides actual values for $\tilde{\omega}_j$; these can be used to study the model performance at a local level and its limitations. With this approach it is possible to circumvent certain technical challenges associated to experimentation. This is particularly valuable in the frame of combustion for liquid rocket engines, where the operating conditions are extreme, limiting the possibilities for experimental measurements. The present paper approaches the challenge of EDC modeling from this perspective. A turbulent flame with conditions relevant to space propulsion applications was simulated using DNS. The results were used to investigate the model performance through a turbulent diffusion flame at high pressure. The high pressures in the combustion chambers of rocket engines decrease the chemical length and timescales. This yields lower Karlovitz numbers and higher Damköhler numbers compared to standard combustion conditions. Such operating conditions may challenge basic assumptions in turbulence theory, such as the forward scattering of Turbulent Kinetic Energy (TKE) [23] or dominance of dissipation in the TKE transport budget [24–26]. Therefore, assessing the validity of conventional models is crucial for understanding their potential and limitations for space propulsion applications.

The rest of the paper is structured as follows. In Section 2, the DNS framework is detailed. In Section 3, the prediction capabilities of EDC are assessed, with a special focus on the regions where discrepancies between the model and observations are largest. The origins of these discrepancies are investigated to unveil the challenges inherent to the EDC application. In addition, the models for the scales of the fine structures are assessed. A special focus is placed on the local variations driven by the Damköhler number and the Reynolds number. Finally, the findings of this paper are summarized in Section 4.

2. Materials and Methods

The present study relies on the analysis of DNS results to investigate the performance of the EDC in modern rocket combustors. This section is devoted to a detailed description of the simulation framework and the subsequent available statistical data.

Two simulation packages were involved in the present work. First, a precursor simulation was used to obtain a physically meaningful incoming turbulent field. This result was then used as an inlet boundary condition in the second domain i.e. the main simulation. The overall strategy is displayed in Figure 1a.

In the precursor simulation, a synthetic velocity field develops into a mature turbulent flow following the strategy described in [27]. The utilized methodology is based on the work of Shur et al. [28]. This approach relies on the superposition of harmonics with randomized amplitudes and phases, following a reference spectrum as originally proposed by Kraichnan [29]. The development into a physically meaningful turbulent flow can be validated using classical second- and higher-order statistical analysis as described in [27]. The characteristic length and velocity scales of the turbulent flow were chosen to match the results obtained from RANS simulations for a scale rocket combustor described in previous works [30]. The turbulence characteristics of the developed flow are summarized in Table 1. It is important to remark that a turbulent diffusion flame is a complex dynamic system. Its structure can dissipate or enhance turbulence through mechanisms not yet completely understood. Hence, local small Reynolds number can arise despite strong inlet turbulent intensity. The analysis of EDC performance in such regions should be conducted with care since large Reynolds numbers is a core assumption for the model application. A numerical simulation of a turbulent diffusion flame ensuring large Reynolds numbers everywhere would imply extremely small minimum Kolmogorov scales, with the subsequent prohibitive computational cost.

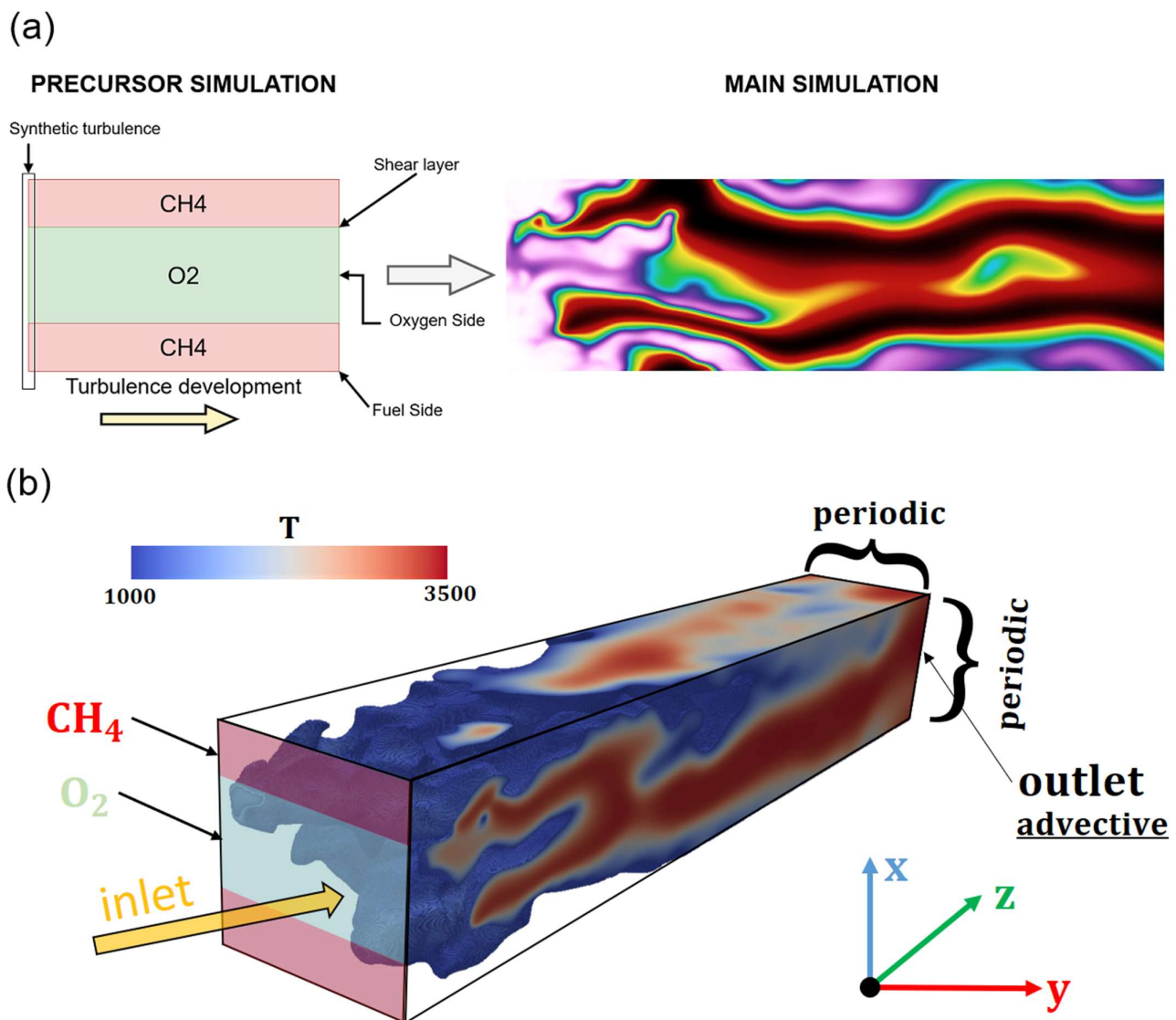


Figure 1. Direct numerical simulation strategy schematic: coupling between the precursor and the main simulation (a), boundary conditions, and the geometry of the main simulation (b).

Table 1. Radially averaged turbulence characteristics at the inlet.

Symbol	Description	Value
Re_L	Reynolds number of the large eddies	348
L	Large eddies scale	87 μm
η	Kolmogorov scale	0.55 μm
u_{rms}	Root mean square of the velocity fluctuations	8 m/s

The main simulation domain is the realm where the turbulent mixing and combustion processes take place. This segment contains the relevant information within the scope of the current work, and it is the one used for post-processing. A standing methane-oxygen diffusion flame was simulated in a cuboid domain with an aspect ratio of roughly 6. Periodic boundary conditions were imposed for all properties in the lateral directions, which are perpendicular to the main flame's propagation direction, as displayed in Figure 1b. The simulated flame aims to represent the turbulent mixing and combustion processes in the

injection region of a rocket combustor. For this reason, the lateral directions are referred to as radial and the main flame propagation direction as axial. Although this terminology is not entirely accurate, it simplifies the discussion and the results' interpretation. The main simulation domain comprises a volume of $0.2 \times 0.2 \times 1.1875$ mm, and it is resolved with $192 \times 192 \times 1140$ cells. The spatial resolution of turbulent and flame structures complies with the main requirements as discussed in [26]. More specifically, the Kolmogorov eddies and the local flame thickness are resolved with at least 0.48 and 10 cells, respectively, at any position. Moreover, the ratio between periodicity and the integral eddies length scale ranges from roughly 4 to 12 through all of the simulated space. This condition ensures a large enough volume to simulate macroscopic turbulence behavior, ensuring ergodicity. Regarding the used solver, the main simulations were carried out using the software EBI (Engler-Bunte-Institute)-DNS [31–34]. This code has been thoroughly validated by several combustion-related studies in recent years [35–39]. EBI-DNS is programmed on the open-source software OpenFOAM [40,41]. In this frame, the conservation equations for mass, momentum, energy, and species are solved using the Finite Volume Method (FVM) [42,43]. Detailed chemistry and transport properties are resolved with Cantera [44], considering the mixture-averaged transport model proposed by Kee et al. [45]. The skeletal mechanism developed by Slavinskaya et al. [46] is used to determine methane combustion using finite rate chemistry. This reaction mechanism was devised for space propulsion applications at high pressures and considered 21 species with roughly 100 reactions. Table 2 presents the relevant combustion parameters for the simulated flame.

Table 2. Combustion parameters.

Scheme	Description	Value
P	Pressure	20 bar
T_R	Temperature of the unburnt reactants	300 K
Φ	Global equivalence ratio	0.5
δ_{L0}	Laminar flame thickness at stoichiometric conditions	5.505 μm
s_{L0}	Laminar flame speed at stoichiometric conditions	2.5735 m/s
s_i/s_{L0}	Normalized bulk velocity of the unburnt gases	3
s_b/s_{L0}	Normalized velocity of the combustion products	31.57

All of the parameters needed for the simulation post-processing were averaged in both time and space. In total, 620 timesteps corresponding to roughly 17 Tb of data were recorded to perform the described statistical analyses. The used data corresponds to 57 eddy turnover times, and 290 times the chemical timescale of the stoichiometric laminar flame ($t_{L0} = \delta_{L0}/s_{L0}$). Such an extensive database ensures the convergence in the statistical parameters. An Average in space can also be performed since the statistics are constant in one of the directions (y in Figure 1). Additional spatial averaging can be conducted, profiting from the flame's symmetric configuration. This consideration allows for the minimization of the final uncertainty in the data. In total, there are $192 \times 2 \times 620 = 238.08 \times 10^3$ observations at each flame position. Using basic statistical inference methods, the final error in the relevant variables can be assessed for each cell. The error is estimated using the width of the interval, within which the actual value falls with a 95% confidence interval. The highest local relative error is in the order of 5%, whilst the spatially averaged error is below 0.5% for every relevant field. Overall, it can be stated that the performed simulation complies with the main quality requirements to be used for turbulence research purposes.

3. Results

This section is devoted to the performance analysis of the EDC combustion model using the results of the described numerical simulations. The study is structured in three different parts. First, the procedure to translate the DNS results into EDC-relevant parameters is described, along with a general overview of the model's error and its origins. The second and third parts address the quality of the models for the fine structures scales.

3.1. EDC Model Performance

At a given position within the DNS solution domain, the EDC assumes that there is a constant g fulfilling the following expression:

$$\tilde{\omega}_j = g \cdot \tilde{\omega}_{j,ps} \quad (6)$$

where $\tilde{\omega}_{j,ps} = (\bar{\rho}/\tau^*) (\tilde{Y}_j^* - \tilde{Y}_j)$ is the pseudo production rate of the j^{th} species. If $\Omega_x \in \mathbb{R}^N$ is used to define a vector containing all the observed pseudo production rates, and $\Omega_y \in \mathbb{R}^N$ denotes the vector containing all the observed average production rates $\tilde{\omega}_j$, then the problem of finding g can be seen as fitting the expression $\Omega_y = g\Omega_x$. The least-squares method yields the following optimal value for g :

$$g = \left(\Omega_x^T W \Omega_x \right)^{-1} \Omega_x^T W \Omega_y \quad (7)$$

where $W \in \mathbb{R}^N$ is a vector containing the weighting factors for each species. These factors can be used to adapt the fitting objective. The pseudo production rate depends on the residence time of the fine structures τ^* which requires the modeling constant C_τ . To approach the problem, we first consider the value originally recommended by Magnussen $C_\tau \approx 0.4082$. Using this constant, the optimal value for g was calculated. This result minimizes the weighted error between the observed and predicted average reaction rates. It can therefore be taken as a reference for the general model performance. It is important to mention that specific weights can be chosen to adapt the error definition. Unit weighting coefficients were chosen within the present work since this option minimizes the local error in species transport. This approach is apt for the present investigation since it addresses the suitability of EDC in the frame of closure for the turbulent transport of species. However, more sophisticated alternatives are feasible. Additional local enhancements in predictability can be achieved through the adaptation of C_τ . Nevertheless, the potential gains are rather moderate through most of the flame. Hence, the model's sensitivity to the coefficient C_τ is omitted here, although it will be addressed in the following section.

The overall model performance can be assessed in Figure 2, where the spatial distribution of the chemical production rates is represented. This result is complemented with the scatter plot in Figure 3, where the observed and predicted values of several species are displayed. As it can be seen, there is a reasonably good agreement for the most prevalent species. However, the model fails in the prediction of the intermediate species, as illustrated in Figure 3.

This figure compares the observed average reaction rates with the EDC outcome. Each point corresponds to one cell in the domain, and their color is related to the mean mixture fraction. The model exhibits different biases depending on whether the average conditions are lean or fuel-rich. In addition, the points with average mixtures close to stoichiometric conditions are prone to present larger discrepancies.

To elucidate the reason behind the observed discrepancies, the turbulent statistics and model execution for the problematic cells were thoroughly studied. The analysis of the carbon monoxide results for a cell in the central region with $z/\delta_{LO} \approx 40$ and $x/\delta_{LO} \approx 3$ is used to illustrate the present research findings. In this particular cell, EDC predicts the negative production of carbon monoxide, whereas DNS observations show a moderate generation. We shall approach the origin of these opposing outcomes by investigating the governing results from within the framework of EDC and the statistics of turbulent combustion.

The sign of the species production predicted by EDC is given by the difference $\tilde{Y}_j^* - \tilde{Y}_j$, which corresponds to the time evolution of a mixture in a PSR with its initial boundary conditions corresponding to the averaged values. This evolution at the considered cell is presented in Figure 4. For the sake of simplicity, only the most relevant species are displayed. As can be seen, most elements present a monotonic behavior with the exception of carbon monoxide (CO). The reason behind this is that the production/destruction of

carbon monoxide in lean combustion at the considered operating conditions is strongly tied to methane availability. Positive production is initially observed through the consumption of oxygen and methane. However, once methane is depleted, carbon dioxide is primarily generated at the expense of both oxygen and the available carbon monoxide i.e., through the global mechanism $2\text{CO} + \text{O}_2 \rightarrow 2\text{CO}_2$. After a certain time, the mass fraction of carbon monoxide can become smaller than the initial one. In such a case, the EDC model will predict negative carbon monoxide production. Whether or not the threshold is reached depends on the parameter C_τ . If values significantly smaller than the recommended one are chosen (i.e., $C_\tau < 0.2$) EDC will predict positive CO generation. However, this sort of adaption lacks physical motivation since smaller time scales of the fine structures do not necessarily cause the overall positive production of carbon monoxide.

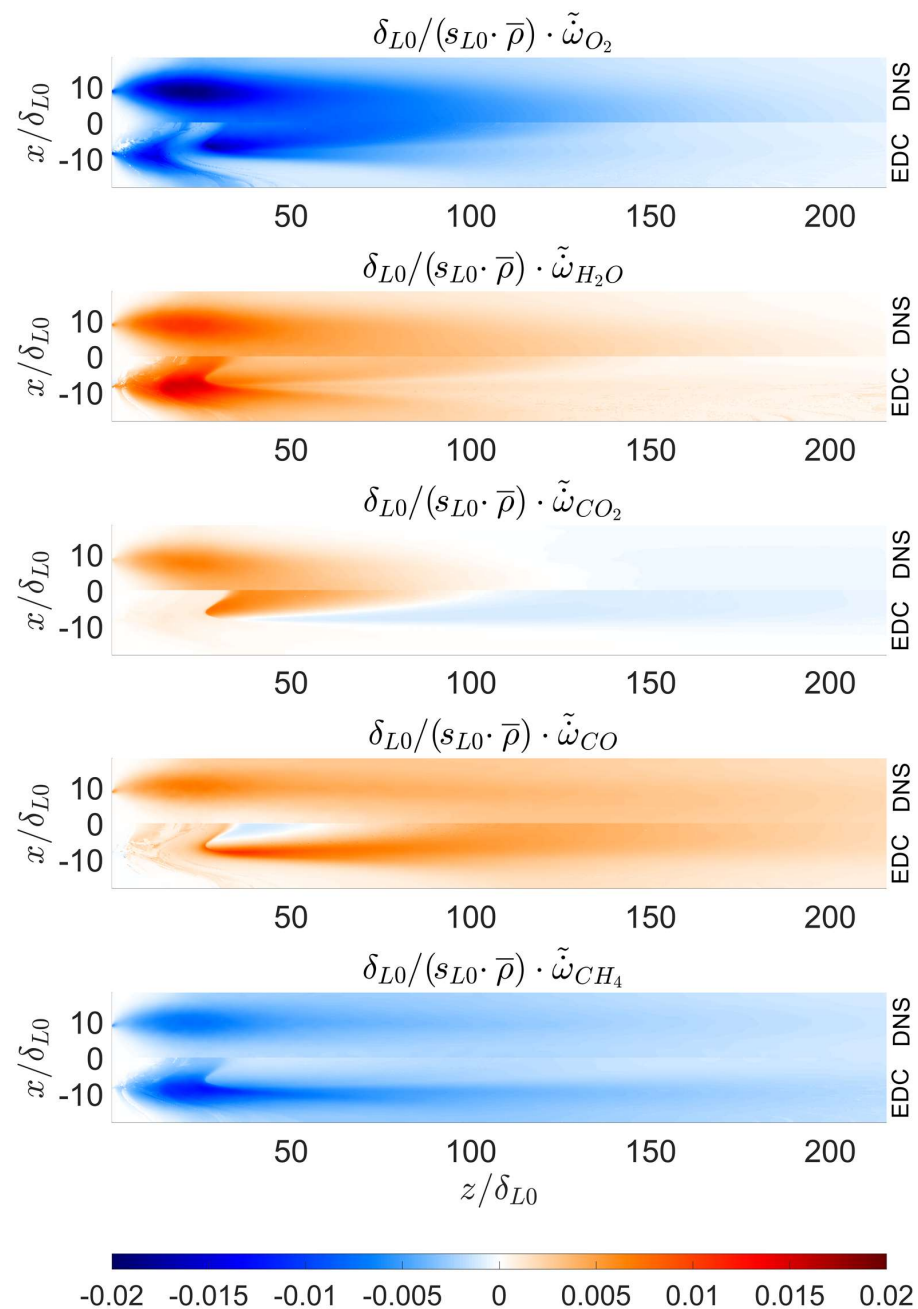


Figure 2. Observed mean chemical production rate in the numerical simulations and the best possible prediction using the Eddy Dissipation Concept.

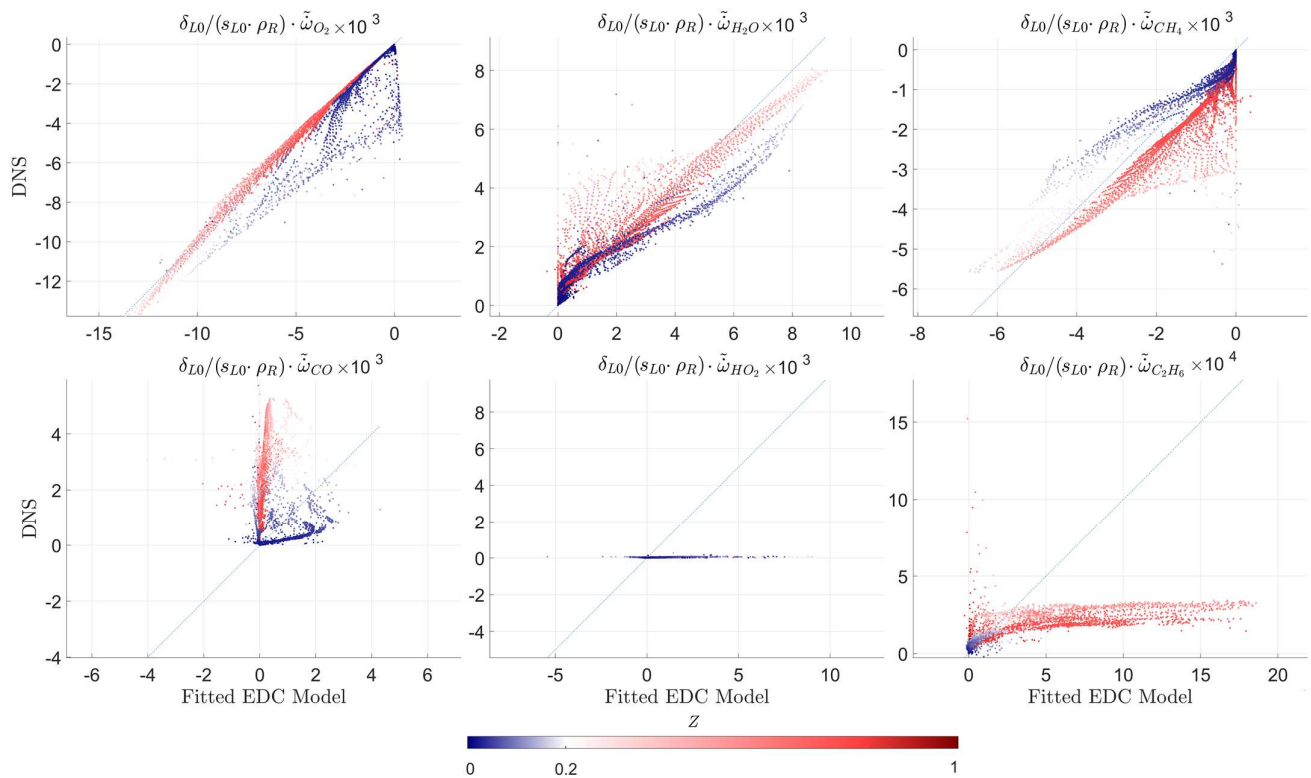


Figure 3. Example of prediction performance of the Eddy Dissipation Concept for different species and $Re_T > 70$.

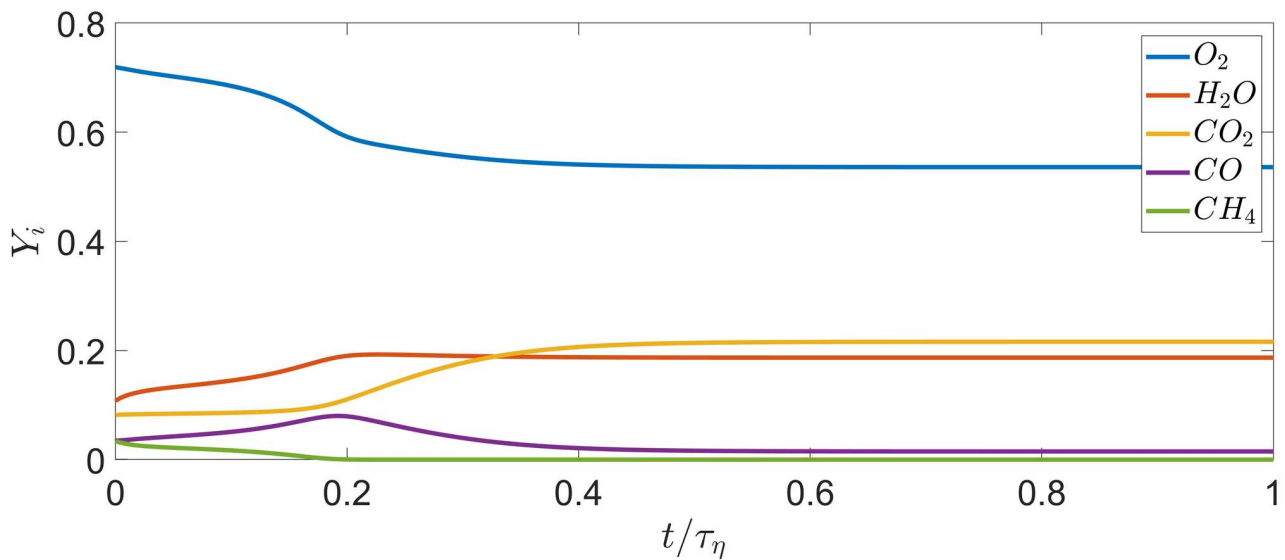


Figure 4. Evolution of the mean concentrations of species over time for a reference cell at $z/\delta_{L0} \approx 40$ and $x/\delta_{L0} \approx 3$.

The next step is to investigate the statistics in the actual turbulent combustion context to unveil the reasons for the overall positive CO generation. As seen in the batch reactor case, the availability of methane constitutes the main driver in the dynamic behavior of carbon monoxide. Hence, the turbulent flame statistics should be studied using the mass concentrations of methane and carbon dioxide as independent variables. The Probability Density Function (PDF) for all the observed combinations of these two species is displayed in Figure 5a. As can be seen, most of the data are concentrated near $\tilde{Y}_{CH4} \approx 0$. This result

is expected since the considered position is very close to the centerline where oxygen is predominant. The PDF is complemented with the observed average mixture fraction for each observed $\tilde{Y}_{CH_4} - \tilde{Y}_{CO}$ combination. The colormap in Figure 5b was chosen to ease the distinction between fuel-rich and lean conditions, with the stoichiometric mixture fraction corresponding to $Z_{st} \approx 0.2$. From these results, the existence of two main regimes, in which combustion occurs is obvious. The upper region corresponds to fuel-rich combustion and is characterized by relatively high concentrations of carbon monoxide. The bottom of Figure 5b denotes the occurrence of combustion in lean conditions, displaying smaller mass fractions of carbon monoxide. In fuel-rich conditions, methane is always available, impairing the global carbon dioxide generation by consuming carbon monoxide and oxygen. Hence, it is reasonable to expect larger mass concentrations of carbon monoxide whenever combustion occurs in fuel-rich conditions.

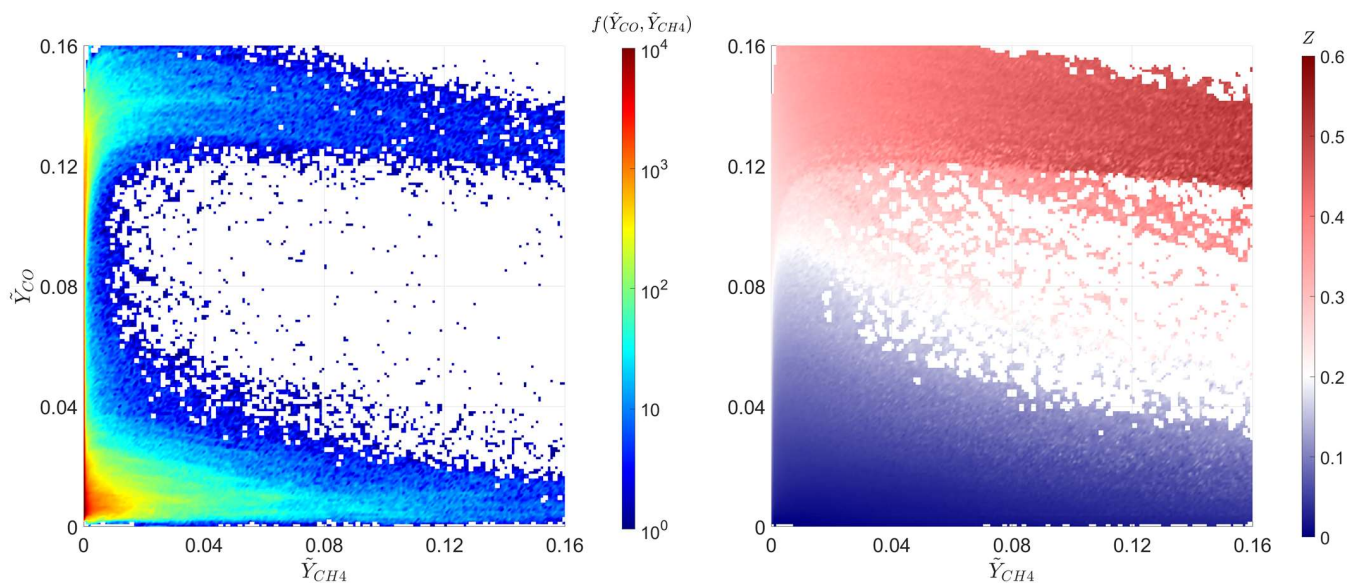


Figure 5. Main combustion regimes in the studied cell: joint probability density function of the mass fractions of methane and carbon monoxide (a), Favre-average mixture fraction as a function of the mass fractions of methane and carbon monoxide (b).

The presence of different combustion regimes cannot be captured in the PSR combustion in which the EDC model is grounded. This effect is rooted in the non-linear effect of turbulent mixing fluctuations in the flame combustion dynamics. Since the mean combustion condition is lean, this is the only considered scenario to determine $\tilde{Y}_j^* - \tilde{Y}_j$. For species with similar behavior in both regimes, the error introduced by the described effect is smaller. Nevertheless, intermediate species and certain final compounds are strongly sensitive to the combustion regime due to their non-monotonic behavior. This variation is the source of the observed discrepancies between EDC and DNS.

The viability of combustion in both rich and lean conditions is the common observed element in the regions where the model performs poorly. Similar analyses can be conducted in other areas where significant deviations between the observed and modeled average reaction rates are reported. Based on these results, we conclude that the challenging predictability arises from the model's incapability to capture the differences in combustion dynamics, as only the more prevalent regime can be considered. Combustion in the context of liquid rocket engines is likely to accentuate these divergences due to the absence of inert elements, widening the mixing conditions in which combustion is viable

3.2. Timescale of the Fine Structures

In this section, the model assumptions concerning the timescales of the fine structures are scrutinized. As previously stated, the fitted value of g depends on C_τ . The physical meaning of this parameter is the timescale of the fine structures compared with that of the Kolmogorov eddies.

For a chosen constant C_τ , at each cell, there is a tuple of predicted and observed values for the mean reaction rates of species. One way to assess the model's overall error is to consider the cumulative relative error for each individual species:

$$E = \sum_{j=1}^n \tilde{Y}_j \frac{2 \cdot |\tilde{\omega}_{j,DNS} - \tilde{\omega}_{j,EDC}|}{|\tilde{\omega}_{j,DNS}| + |\tilde{\omega}_{j,EDC}|} \quad (8)$$

where the Favre-averaged mass fraction \tilde{Y}_j is used to weight each individual error. The obtained value in (8) enables an estimation of the model's discrepancy with the DNS observations. To assess the influence of the constant C_τ in the error performance, the sensitivity coefficient of E with respect to C_τ is determined:

$$E_{C_\tau} = \frac{\partial E}{\partial C_\tau} \quad (9)$$

Therefore, values close to zero indicate that the reference value for C_τ is near a local optimum. Likewise, negative, and positive values indicate that the reference constant is above and below the local optimum respectively. It is possible to determine this parameter numerically after evaluating the model's error with two different values of C_τ , and using finite differences. The result of this calculation is presented in Figure 6 for $C_\tau = 1$. This value was chosen to fall within the recommended margins, as stated by Ertesvåg [47].

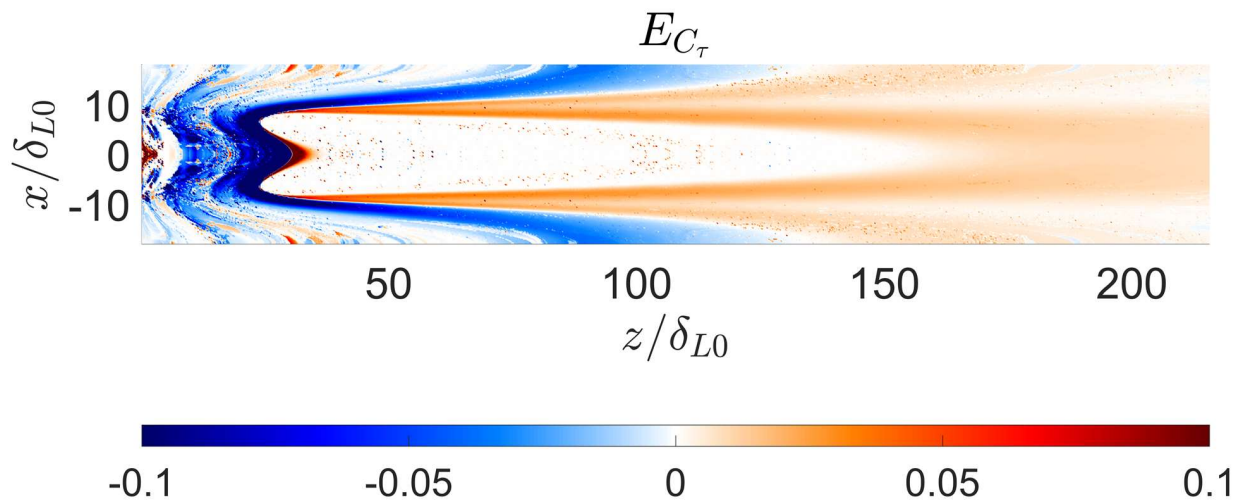


Figure 6. Model error sensitivity to the factor C_τ at $C_\tau = 1$.

The obtained graph displays consistent trends in accordance with the progress of the turbulent combustion process. At the flame's core, the error presents no sensitivity to the factor C_τ . Negative values can be found in the outer region of the shear layer, whereas positive values appear in the lean part of the reactive shear layer and further downstream.

The low sensitivity at the core is likely to be caused by the coexistence of both lean and fuel-rich regimes, as previously discussed. This circumstance impairs the overall quality of the EDC application. Hence, the performance sensitivity to model parameters decreases due to the increased noise levels. Moreover, the Reynolds number is very small in this region, and the basic assumption of a turbulent flow may be challenged. In such a context, the overall application of EDC is likely to be additionally hindered. Ideally, the inlet turbulent

intensity would be high enough to ensure high Reynolds numbers in the entire domain. However, this would incur prohibitive computational costs. The fine structures appear to have larger timescales compared to Kolmogorov on the lean side. This result is probably caused by the asymmetrical behavior of the flame dynamics with respect to stoichiometric conditions. In high-pressure laminar methane-oxygen flames, the chemical timescale grows faster towards lean than in fuel-rich conditions [48]. Assuming that the combustion dynamics of fine structures follow a similar trend, it is reasonable to expect larger timescales in lean regions than in fuel-rich areas. In the region further downstream, the conditions are almost entirely fuel-rich, with the sensitivity coefficient E_{C_τ} being predominantly positive. These positive values are likely related to the longer chemical timescales, as previously mentioned. Parente et al. [11] and Bao [12] formalized the local variations of C_τ depending on turbulence and chemical conditions. In their work, dependencies of the coefficient C_τ on the Damköhler number and the Reynolds number were discussed. Both research groups deduced a proportionality law of $C_\tau \sim 1/(Da_\eta \sqrt{Re_T + 1})$. Hence, the timescale of the fine structures increases with decreasing values of Da_η and Re_T . To investigate the validity of these results within the present context, these two dimensionless numbers were calculated. The chemical timescale was determined using the following formula, which considers the contribution of all species:

$$t_c = \sum_{j=1}^n Y_j \frac{\bar{p}_j}{|\tilde{\omega}_{j,DNS}|} \quad (10)$$

The spatial field for both dimensionless numbers is displayed in Figure 7. As can be seen, the regions with high values of Da_η and Re_T seem to correspond with areas where $E_{C_\tau} > 0$, indicating that the ideal value for C_τ is lower than the reference one. This result concurs with the trends discussed in the works of Parente et al. and Bao.

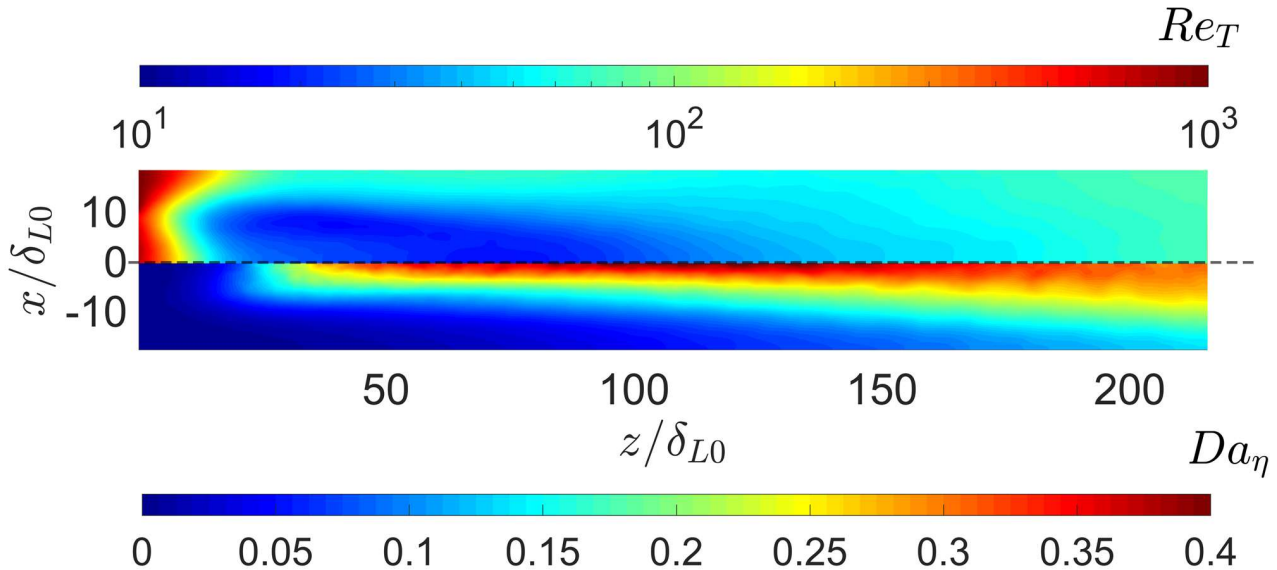


Figure 7. Relevant dimensionless numbers at the simulated flame: local turbulent Reynolds number (top), local Damköhler number of the Kolmogorov eddies (bottom).

To investigate the dependency law $C_\tau \sim 1/(Da_\eta \sqrt{Re_T + 1})$ in greater detail, the error sensitivity E_{C_τ} is plotted against this factor in Figure 8. Although the dispersion of the recorded data is significant, the expected growth trend is observed. The relatively large amount of dispersion can be caused by the result's high sensitivity to the definitions used for the model error E and chemical timescales t_c . In any case, it is quite evident that the optimal value for C_τ grows with $1/(Da_\eta \sqrt{Re_T + 1})$.

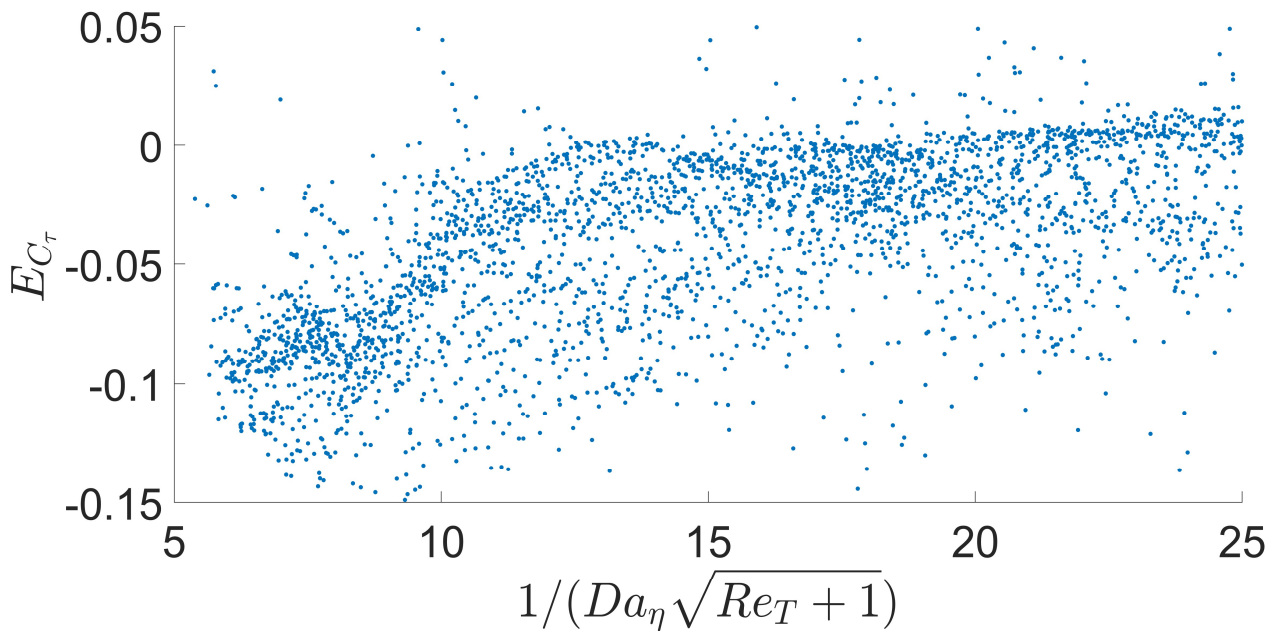


Figure 8. Model sensitivity to C_τ as a function of $1/(Da_\eta\sqrt{Re_T + 1})$.

3.3. Lengthscale of the Fine Structures

The other relevant degree of freedom in EDC is the constant C_γ , which is used to determine the volumetric fraction of the fine structures. Approaching this parameter is far more convoluted due to its dependency on the version-specific exponents n m and the factor χ . In the present sub-section, the behavior of this coefficient is investigated using the values for g obtained with the post-processing strategy described above.

The most immediate hindrance to determining the coefficient C_γ are the coefficients n and m in (5). These exponents are integers ranging from 2 to 3. Hence, it is always possible to analytically solve γ_λ for g and χ for any combination of n and m . Nevertheless, for the cases in which $m \neq n$ the resulting equation is a third-degree polynomial whose analytical solution presents a challenging interpretation. Contrarily, the cases $m = n$ accept a simple solution of the form:

$$\gamma_{\lambda,mm} = \sqrt[n]{\frac{g}{\chi(1+g)}} \quad (11)$$

where $\gamma_{\lambda,mm}$ denotes the solution for generic values of m and n . The solutions for $n = m = 2$ and $n = m = 3$ can easily be determined using this equation. The other possible combinations i.e. $\gamma_{\lambda,23}$ and $\gamma_{\lambda,32}$ must forcibly lead to results that fall between $\gamma_{\lambda,22}$ and $\gamma_{\lambda,33}$. For these reasons, the results $\gamma_{\lambda,22}$ and $\gamma_{\lambda,33}$ can be taken as a reference for the minimum and maximum thresholds, within which the volumetric fraction of fine structures must fall. Therefore, the study can be restricted to these limit cases since they indicate bounds for the actual values. Following this approach, the coefficient C_γ can be estimated as:

$$C_{\gamma,mm} = \frac{Re_T^{-\frac{1}{4}}}{\gamma_\lambda} = \frac{Re_T^{-\frac{1}{4}}}{\gamma_\lambda} = \frac{Re_T^{-\frac{1}{4}}}{\sqrt[n]{g/(1+g)}} \sqrt[n]{\chi} \quad (12)$$

At this point, the factor of reacting fine structures χ hinders the completion of the analysis. To circumvent this issue, a value $\chi = 1$ is initially assumed. The corresponding value can be taken as a ceiling for the actual coefficient since $\chi \leq 1$. This upper value is denoted as C_γ^0 and it was calculated at all the flame positions. The probability density function for all the observed values C_γ^0 is displayed in Figure 9. As can be seen, most of the data are concentrated at $C_\gamma \approx 1.8$ for $n = m = 2$ and $C_\gamma \approx 2.2$ for $n = m = 3$. This

outcome is in good agreement with EDC theory [13], since the values obtained using (12) should lie between 0 and the reference value $C_{\gamma,ref} \approx 2.14$.

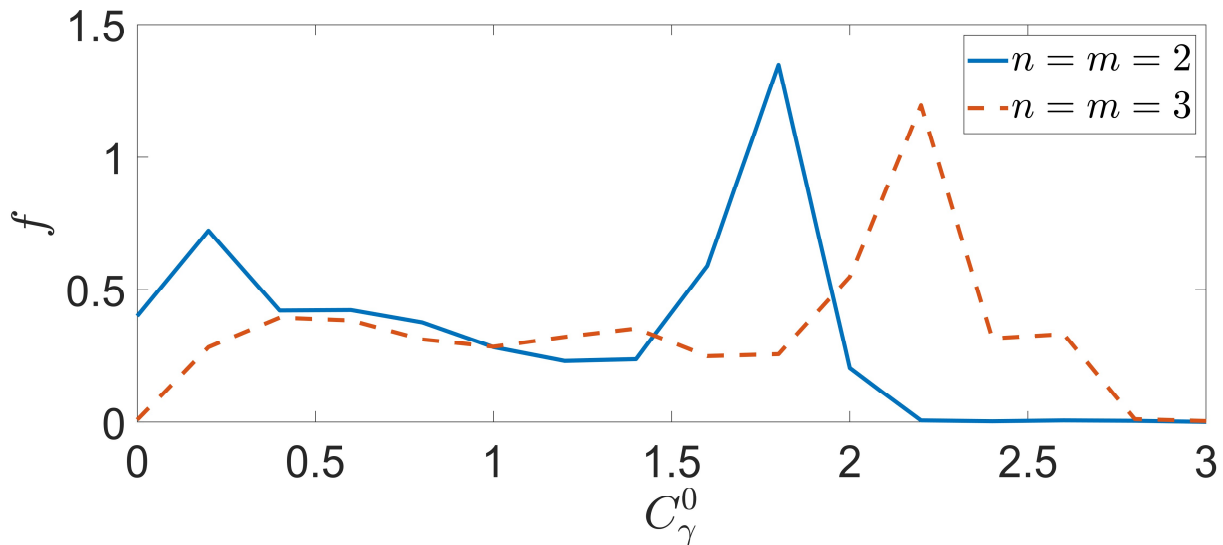


Figure 9. Probability Density Function of the observed coefficient C_{γ}^0 .

In the context of EDC theory, the observed values below $C_{\gamma,ref}$ can be caused by two main factors. First, the fraction of the reacting fine structures χ can be below unity. Second, the reference $C_{\gamma,ref}$ is not constant but depends on the Damköhler number and the Reynolds number. These possibilities shall be evaluated using the available data. An initial estimation of the fraction of reacting fine structures can be shown as:

$$\chi_{nm} = \sqrt[n]{\frac{C_{\gamma,ref}}{C_{\gamma,nm}^0}} \quad (13)$$

This result is tied to the assumption that the offset between $C_{\gamma,nm}^0$ and the reference value is entirely caused by the presence of non-reacting fine structures. Hence, values above unity indicate that the value $C_{\gamma,ref}$ must necessarily be larger than the recommended one. Unlike in the case of C_{τ} , different dependency laws have been derived. Parente proposed a law in the order $C_{\gamma} \sim \sqrt{(Re_T + 1)Da_{\eta}}$ whilst Bao deduced a relationship of the sort $C_{\gamma} \sim \sqrt{(Re_T + 1)Da_{\eta}^3}$. Figure 10 was elaborated to investigate the validity of these dependencies in the present case. The fraction of reacting fine structures tends towards zero for the extreme values of the Favre-averaged mixture fraction \tilde{Z} . This result is expected since the likeliness of falling outside the flammability limits increases as $\tilde{Z} \approx 0$ and $\tilde{Z} \approx 1$.

Both graphs present a significant amount of points with $\chi_{nm} > 1$. These recorded data can only be attributed to the fact that the actual coefficient C_{γ} is higher than the reference value.

The elaborated graphs allow us to study the dependency on Da_{η} and Re_T . As it can be seen, the Damköhler number of the Kolmogorov eddies increases as points move further away from unity χ_{nm} . This tendency implies that the required value of C_{γ} increases with growing Da_{η} , as suggested by Parente et al. and Bao. Nevertheless, the predicted effect of the Reynolds number cannot be appreciated in the present research. Indeed, a weak inverted trend can be noticed. This result could be caused by a weak coupling between Da_{η} and Re_T . In regions where chemical reactions are scarce, the viscosity is higher due to the higher prevalence of reactants, yielding larger Reynolds numbers. This effect causes a weak decreasing trend of Re_T with Da_{η} . Nevertheless, due to the low correlation it is difficult to unveil the causes behind the mentioned outcome.

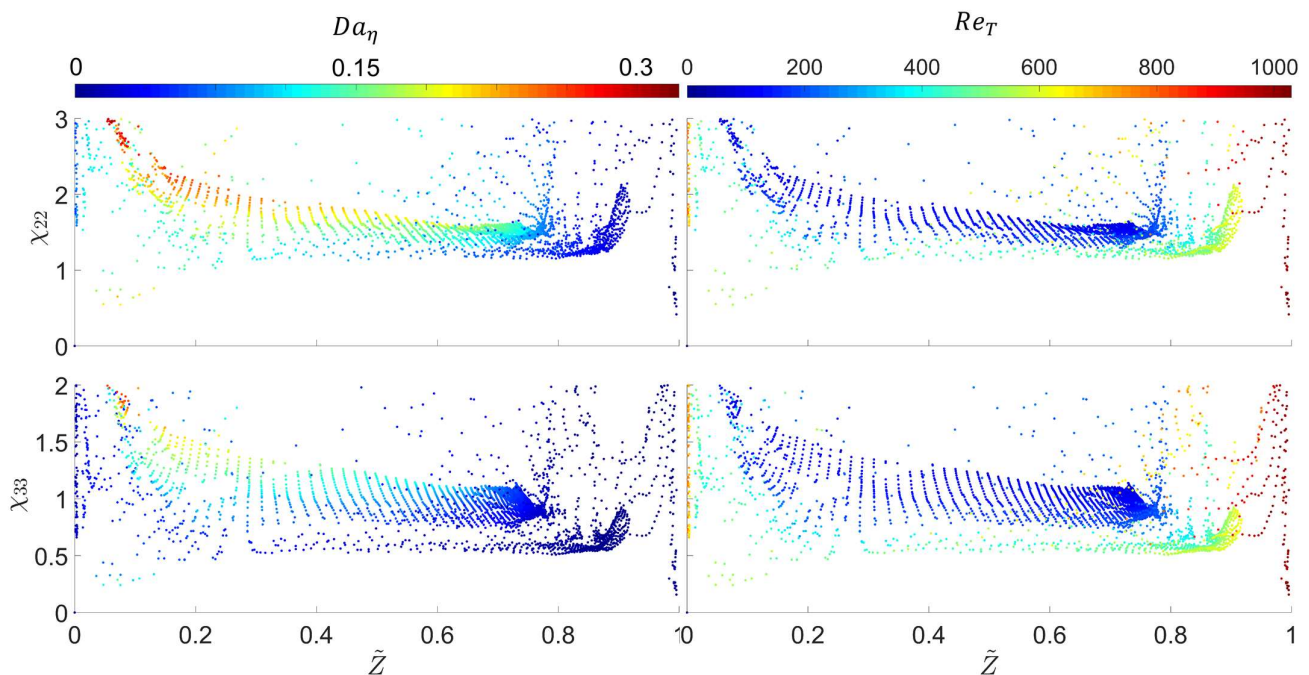


Figure 10. Estimated values for χ_{nm} as a function of the Favre-averaged mixture fraction \tilde{Z} , the Damköhler number of the Kolmogorov eddies Da_η , and the turbulent Reynolds number Re_τ for $Re_\tau > 70$.

4. Discussion

Direct numerical simulations of a high-pressure turbulent diffusion flame were used to investigate the suitability of EDC for space propulsion combustion applications. The model appeared to be able to predict the mean production of species for the large components with good performance. However, significant discrepancies between the model and observations were reported for intermediate species. The authors hypothesize that these inconsistencies are driven by the fact that average mass fractions cannot capture the intermittency of combustion between lean and fuel-rich regimes. This claim is based on the observed positive carbon monoxide generation in regions with mean lean mixtures. Such a behavior originates from the turbulent fluctuations of the mixing conditions, and it cannot be captured with 0D reactor approaches. The models for the fine structures' scales were additionally assessed. The coefficient C_τ appeared to vary with the Damköhler number and the Reynolds number, in keeping with the trends predicted in recent studies. The behavior of the parameter C_γ was also addressed. This parameter seemed to be sensitive to the Damköhler number, although no relationship with the Reynolds number was found.

In general terms, EDC is able to predict the mean production rate of the most prevalent species with moderate accuracy. For intermediate species, the model's capabilities seem to be rather poor. This condition may limit the benefits of using detailed chemical mechanisms since the errors in the transport of intermediate components may propagate to the principal combustion products. Furthermore, the standard models for the characterization of the fine structures are not able to capture strong local variations. Adaption for these formulations is required to exploit the EDC's capabilities. Hence, model extensions are recommended to enhance the quality of EDC for its usage in space propulsion applications. One possibility for enhancing the EDC performance would be to incorporate higher order statistics for the determination of the fine structures' chemistry. Hence, instead of restricting the analysis to mean conditions, the reaction rates calculations could be split for different mixing conditions.

Author Contributions: Conceptualization, D.M.-S.; methodology, D.M.-S.; software, D.M.-S. and A.S.; validation, O.H., X.H. and A.S.; formal analysis, D.M.-S.; investigation, D.M.-S. and J.S.; resources, A.S. and J.S.; data curation, D.M.-S.; writing—original draft preparation, D.M.-S.; writing—review and editing, D.M.-S., O.H. and X.H.; visualization, D.M.-S.; supervision, O.H.; project administration, O.H.; funding acquisition, O.H. and A.S. All authors have read and agreed to the published version of the manuscript.

Funding: This research was funded by the Bayerische Forschungsförderung (BFS), “Weiterentwicklung der CFD-Simulationsmethoden für H₂-O₂-Hochdruck-Dampfgeneratoren zur Stromnetzstabilisierung” Projektnummer: AZ-1517-21.

Data Availability Statement: The authors will share the used datasets upon reasonable request.

Acknowledgments: The authors thank SuperMUC-NG for providing the computational resources for performing the numerical simulations. In addition, the authors are extremely grateful to Martin Ohlerich for his availability and technical support.

Conflicts of Interest: The authors declare no conflict of interest.

References

- Haidn, O.J. *Advanced Rocket Engines*; Lampoldshausen, Germany. 2008. Available online: <https://www.macro-inc.com/NASADocs/AdvanceRocketEnginesEN-AVT-150-06.pdf> (accessed on 20 July 2022).
- Huzel, D.K.; Huang, D.H. *Modern Engineering for Design of Liquid-Propellant Rocket Engines*; American Institute of Aeronautics and Astronautics: Reston, VA, USA, 1992; pp. 67–134.
- Biblarz, O.; Sutton, G.P. *Rocket Propulsion Elements, 9th ed*; Wiley: Hoboken, NJ, USA, 2017.
- Ivancic, B.; Riedmann, H.; Frey, M.; Knab, O.; Karl, O.; Hannemann, K. Investigation of Different Modeling Approaches for CFD Simulation of High Pressure Rocket Combustors. In Proceedings of the 5th European Conference for Aeronautics and Space Sciences (EUCASS), Munich, Germany, 1–5 July 2013.
- Pope, S.B. *Turbulent Flows*; Cambridge University Press: Cambridge, UK, 2000.
- Favre, A. *Problems of Hydrodynamics and Continuum Mechanics*; SIAM: Philadelphia, PA, USA, 1969.
- Peters, N. Laminar Flamelet Concepts in Turbulent Combustion. *Twenty-First Symp. (Int.) Combust.* **1986**, *21*, 1231–1250. [[CrossRef](#)]
- Magnussen, B.F.; Hjertager, B.H. On Mathematical Modeling of Turbulent Combustion with Special Emphasis on Soot Formation and Combustion. *Symp. (Int.) Combust.* **1977**, *16*, 719–729. [[CrossRef](#)]
- Magnussen, B.F.; Hjertager, B.H.; Olsen, J.G.; Bhaduri, D. Effects of Turbulent Structure and Local Concentrations on Soot Formation and Combustion in C₂H₂ Diffusion Flames. *Symp. (Int.) Combust.* **1979**, *17*, 1383–1393. [[CrossRef](#)]
- Magnussen, B.F. On the Structure of Turbulence and a Generalized Eddy Dissipation Concept for Chemical Reaction in Turbulent Flow. In Proceedings of the 19th Aerospace Sciences Meeting, St. Louis, MO, USA, 12–15 January 1981.
- Parente, A.; Malik, M.R.; Contino, F.; Cuoci, A.; Dally, B.B. Extension of the Eddy Dissipation Concept for turbulence/chemistry interactions to MILD combustion. *Fuel* **2016**, *163*, 98–111. [[CrossRef](#)]
- Bao, H. Development and Validation of a New Eddy Dissipation Concept (EDC) Model for MILD Combustion. Master’s Thesis, Delft University of Technology, Delft, The Netherlands, 2017.
- Magnussen, B.F. The Eddy Dissipation Concept—A Bridge between Science and Technology. In Proceedings of the ECCOMAS Thematic Conference on Computational Combustion, Lisbon, Portugal, 21–24 June 2005.
- Ertesvåg, I.S. Analysis of some Recently Proposed Modifications to the Eddy Dissipation Concept (EDC). *Combust. Sci. Technol.* **2020**, *192*, 1108–1136. [[CrossRef](#)]
- Bösenhofer, M.; Wartha, E.-M.; Jordan, C.; Harasek, M. The Eddy Dissipation Concept—Analysis of Different Fine Structure Treatments for Classical Combustion. *Energies* **2018**, *11*, 1902. [[CrossRef](#)]
- Shvab, J. Numerical Investigation of the Combustion Process in a Sub Scale GCH₄/GOX Combustion Chamber with the Usage of the Eddy-Dissipation-Concept Model. Semester Thesis, Technical University of Munich, Munich, Germany, 2018.
- Lewandowski, M.T.; Ertesvåg, I.S. The Impact of the Fine Structure Reactor Formulation in the Eddy Dissipation Concept for MILD Combustion Modelling. In Proceedings of the 11th ERCOFTAC Engineering, Turbulence, Modelling and Measurement, Palermo, Italy, 21–23 September 2016.
- Lewandowski, M.T.; Ertesvåg, I.S.; Pozorski, J. Influence of the Reactivity of the Fine Structures Modeling of the Jet-In-Hot-Coflow Flames with the Eddy Dissipation Concept. In Proceedings of the 8th European Combustion Meeting, Dubrovnik, Croatia, 18–21 April 2017.
- Gran, I.R. Mathematical Modeling and Numerical Simulation of Chemical Kinetics in Turbulent Combustion. Ph.D. Thesis, Norwegian University of Science and Technology, Trondheim, Norway, 1994.
- Gran, I.R.; Magnussen, B.F. A Numerical Study of a Bluff-body Stabilized Diffusion Flame. Part 2. Influence of Combustion Modeling and Finite-rate Chemistry. *Combust. Sci. Technol.* **1996**, *119*, 191–217. [[CrossRef](#)]
- AIAA. *Guide for the Verification and Validation of Computational Fluid Dynamics Simulations*; American Institute of Aeronautics and Astronautics: Reston, VA, USA, 1998.

22. Oberkampf, W.L.; Trucano, T.G. Verification and Validation in Computational Fluid Dynamics. *Prog. Aerosp. Sci.* **2002**, *38*, 209–272. [[CrossRef](#)]
23. Towery, C.A.Z.; Poludnenko, A.Y.; Urzay, J.; O'Brien, J.; Ihme, M.; Hamlington, P.E. Spectral Kinetic Energy Transfer in Turbulent Premixed Reacting Flows. *Phys. Rev.* **2016**, *E93*, 053115. [[CrossRef](#)]
24. Chakraborty, N.; Katragadda, M.; Cant, R.S. Statistics and Modelling of Turbulent Kinetic Energy Transport in Different Regimes of Premixed Combustion. *Flow Turbul. Combust.* **2011**, *87*, 205–235. [[CrossRef](#)]
25. Chakraborty, N. Influence of Thermal Expansion on Fluid Dynamics of Turbulent Premixed Combustion and its Modelling Implications. *Flow Turbul. Combustion* **2021**, *106*, 753–848. [[CrossRef](#)]
26. Martínez-Sanchis, D.; Banik, S.; Sternin, A.; Sternin, D.; Haidn, O.; Tajmar, M. Analysis of Turbulence Generation and Dissipation in Shear Layers of Methane-oxygen Diffusion Flames using Direct Numerical Simulations. *Phys. Fluids* **2022**, *34*, 045121. [[CrossRef](#)]
27. Martínez-Sanchis, D.; Sternin, A.; Sternin, D.; Haidn, O.; Tajmar, M. Analysis of Periodic Synthetic Turbulence Generation and Development for Direct Numerical Simulations. *Phys. Fluids* **2021**, *33*, 125130. [[CrossRef](#)]
28. Shur, M.L.; Spalart, P.R.; Strelets, M.K.; Travin, A.K. Synthetic Turbulence Generators for RANS-LES Interfaces in Zonal Simulations of Aerodynamic and Aeroacoustic Problems. *Flow Turbul. Combust.* **2014**, *93*, 63–92. [[CrossRef](#)]
29. Kraichnan, R.H. Diffusion by a Random Velocity Field. *Phys. Fluids* **1970**, *13*, 23–31. [[CrossRef](#)]
30. Sternin, A.; Perakis, N.; Celano, M.P.; Haidn, O. CFD-analysis of the Effect of a Cooling Film on Flow and Heat Transfer Characteristics in a GCH4/GOX rocket Combustion Chamber. In Proceedings of the Space Propulsion 2018, Sevilla, Spain, 14–18 May 2018.
31. Zhang, F.; Bonart, H.; Zirwes, T.; Habisreuther, P.; Bockhorn, H.; Zarzalis, N. Direct numerical simulation of chemically reacting flows with the public domain code OpenFOAM. In *High Performance Computing in Science and Engineering '14*; Nagel, W.E., Kröner, D.H., Resch, M., Eds.; Springer: Cham, Germany, 2015; Volume 14, pp. 221–236.
32. Zirwes, T.; Zhang, F.; Denev, J.; Habisreuther, P.; Bockhorn, H. Automated Code Generation for Maximizing Performance of Detailed Chemistry Calculations in OpenFOAM. In *High Performance Computing in Science and Engineering '17*; Nagel, W.E., Kröner, D.H., Resch, M., Eds.; Springer: Cham, Germany, 2018; pp. 189–204.
33. Zirwes, T.; Zhang, F.; Denev, J.A.; Habisreuther, P.; Bockhorn, H.; Trimis, D. Improved Vectorization for Efficient Chemistry Computations in OpenFOAM for Large Scale Combustion Simulations. In *High Performance Computing in Science and Engineering '18*; Nagel, W.E., Kröner, D.H., Resch, M.M., Eds.; Springer: Cham, Germany, 2019; pp. 209–224.
34. Zirwes, T.; Zhang, F.; Habisreuther, P.; Denev, J.A.; Bockhorn, H.; Trimis, D. Implementation and Validation of a Computationally Efficient DNS Solver for Reacting Flows in OpenFOAM. In Proceedings of the 14th World Congress on Computational Mechanics, Virtual Congress, 11–15 January 2021.
35. Zhang, F.; Zirwes, T.; Nawroth, H.; Habisreuther, P.; Bockhorn, H.; Paschereit, C.O. Combustion-generated Noise: An Environment-related Issue for Future Combustion Systems. *Energy Technol.* **2017**, *5*, 1045–1054. [[CrossRef](#)]
36. Zhang, F.; Zirwes, T.; Habisreuther, P.; Bockhorn, H. Effect of Unsteady Stretching on the Flame Local Dynamics. *Combust. Flame.* **2017**, *175*, 170–179. [[CrossRef](#)]
37. Zirwes, T.; Häber, T.; Feichi, Z.; Kosaka, H.; Dreizler, A.; Steinhausen, M.; Hasse, C.; Stagni, A.; Trimis, D.; Suntz, R.; et al. Numerical Study of Quenching Distances for Side-wall Quenching Using Detailed Diffusion and Chemistry. *Flow Turbul. Combust.* **2021**, *106*, 649–679. [[CrossRef](#)]
38. Zhang, F.; Zirwes, T.; Häber, T.; Bockhorn, H.; Trimis, D.; Suntz, R. Near Wall Dynamics of Premixed Flames. *Proc. Combust. Institute* **2021**, *38*, 1955–1964. [[CrossRef](#)]
39. Zirwes, T.; Zhang, F.; Habisreuther, P.; Hansinger, M.; Bockhorn, H.; Pfitzner, M.; Trimis, D. Quasi-DNS Dataset of a Piloted Flame with Inhomogeneous Inlet Conditions. *Flow Turbul. Combust.* **2019**, *104*, 997–1027. [[CrossRef](#)]
40. Weller, H.; Tabor, G.; Jasak, H.; Fureby, C. A Tensorial Approach to Computational Continuum Mechanics Using Object-oriented Techniques. *Comput. Phys.* **1998**, *12*, 620–631. [[CrossRef](#)]
41. Weller, H.; Tabor, G.; Jasak, H.; Fureby, C. *OpenFOAM*, version 5.0; openCFD Ltd.: Bracknell, UK, 2017.
42. McDonald, P.W. The Computation of Transonic Flow Through Two-dimensional Gas Turbine Cascades. In Proceedings of the ASME 1971 International Gas Turbine Conference and Products Show, Houston, TX, USA, 28 March–1 April 1971.
43. MacCormack, R.W.; Paullay, A.J. Computational Efficiency Achieved by Time Splitting of Finite Difference Operators. In Proceedings of the 10th Aerospace Sciences Meeting, San Diego, CA, USA, 17–19 January 1972.
44. Goodwin, D.G.; Moffat, H.K.; Speth, R.L. Cantera: An Object-oriented Software Toolkit for Chemical Kinetics, Thermodynamics and Transport Processes Version 2.3.0b. 2017. Available online: <https://zenodo.org/record/170284#YwmFNRxBxZV> (accessed on 24 August 2022).
45. Kee, R.; Coltrin, M.; Glarborg, P. *Chemically Reacting Flow: Theory and Practice*. Wiley: Hoboken, NJ, USA, 2005.
46. Slavinskaya, N.; Abbasi, M.; Starcke, J.H.; Haidn, O. Methane Skeletal Mechanism for Space Propulsion Applications. In Proceedings of the 52nd AIAA/SAE/ASEE Joint Propulsion Conference, Salt Lake City, UT, USA, 25–27 July 2016.
47. Ertesvåg, I.S. Scrutinizing Proposed Extensions to the Eddy Dissipation Concept (EDC) at Low Turbulence Reynolds Numbers and Low Damköhler Numbers. *Fuel* **2022**, *309*, 122032. [[CrossRef](#)]
48. Martínez-Sanchis, D. A Flame Control Method for Direct Numerical Simulations of Reacting Flows in Rocket Engines. Master's Thesis, Technical University of Munich, Munich, Germany, 2021.